EARTH SCIENCES
RESEARCH JOURNAL
Earth Sci. Res. J. Vol. 29, No. 1 (March, 2025): 81 - 88

UNIVERSIDAD NACIONAL DE COLOMBIA

GEOPHYSICS

A comparative study of vertical geoelectrical arrays in delineating shallow subsurface properties

Risky Martin Antosia
Department of Geophysical Engineering, Sumatera Institute of Technology,
Jalan Terusan Ryacudu, Way Huwi, Jati Agung, Kabupaten Lampung Selatan, Lampung, Indonesia.
Email: martin.antosia@tg.itera.ac.id

ABSTRACT

The geoelectrical method, particularly the vertical resistivity technique, is extensively utilized in numerous studies, especially for groundwater exploration and analysis. Predominantly, the Schlumberger (SC) array is employed in these applications. This study seeks to identify an alternative electrode configuration for delineating subsurface features and to effectively compare various electrode arrangements within the one-dimensional (1D) technique. In addition to the SC array, this research evaluates the classical Wenner Alpha (WA), Wenner Beta (WB), and dipole-dipole (DD) arrays. Over a measurement length of approximately 100 meters, the WB and SC arrays demonstrated preferable delineation of subsurface properties compared to the others. These arrays exhibited enhanced performance in signal strength, vertical sensitivity and resolution, and depth of investigation. Therefore, in addition to the SC array, the WB array serves as a viable alternative for vertical geoelectrical surveys. Nonetheless, further studies with extended measurement ranges are necessary to confirm these findings and assess their applicability in larger-scale surveys.

Keywords: geoelectrical method, vertical resistivity technique, Schlumberger, Wenner Alpha, Wenner Beta, dipole-dipole.

Estudio comparativo de matrices geoeléctricas verticales para delinear características bajo la superficie

RESUMEN

Los métodos geoeléctricos, particularmente el sondeo eléctrico vertical, se utilizan ampliamente en diversos estudios, especialmente en la exploración y análisis de aguas subterráneas. La matriz de Schlumberger predomina en estas aplicaciones. Este estudio busca identificar una configuración de electrodos alternativa para delinear las características bajo la superficie y para comparar efectivamente varias configuraciones de electrodos dentro de la técnica unidimensional. Además de la matriz de Schlumberger, este artículo evalúa las clásicas matrices de Wenner Alpha, Wenner Beta y dipolo-dipolo. En una medición de aproximadamente 100 metros de longitud las matrices de Wenner Beta y de Schlumberger mostraron delineaciones preferibles de propiedades bajo la superficie en comparación con las otras. Estas matrices mostraron desempeño mejorado en fortaleza de señal, sensibilidad vertical y resolución y profundidad de la investigación. Además de la matriz de Schlumberger, la matriz de Wenner Beta sirve como una alternativa viable para los sondeos verticales geoeléctricos. Sin embargo, se necesitan estudios con mayores rangos de medida para confirmar estos hallazgos y medir su aplicabilidad en sondeos a mayor escala.

Palabras Claves: método geoeléctrico; técnica de resistividad vertical; Schlumberger; Wenner Alpha; Wenner Beta; dipolo-dipolo

Manuscript received: 23/05/2023
Accepted for publication: 26/02/2025

How to cite
Antosia, R. M. (2025). A comparative study of vertical geoelectrical arrays in delineating shallow subsurface properties. *Earth Sciences Research Journal, 29*(1), 81-88. https://doi.org/10.15446/esrj.v29n1.109067

ISSN 1794-6190 e-ISSN 2339-3459
https://doi.org/10.15446/esrj.v29n1.109067

1. Introduction

Over the past decades, numerous studies have employed the geoelectrical method to investigate the Earth's subsurface. This technique measures potential differences between two electrodes resulting from electrical currents passing through the subsurface (Dentith & Mudge, 2014; Lowrie, 2007; Reynolds, 2011). The electrical resistivity is determined using the inversion method, a key subsurface property that can subsequently be interpreted to infer various geological features. For instance, geoelectrical methods can provide insights into landslide-prone areas (Rezaei et al., 2018), fractured zones (Ojo et al., 2011), underground cavities (Amini & Ramazi, 2017; Farooq et al., 2012), and weak geological zones (Al-Saady et al., 2022). Additionally, this method is widely recognized for its applications in natural resource exploration, including mineral prospecting (Antosia et al., 2021; Arifin et al., 2019; Farduwin et al., 2021; Fernandes et al., 2018) and groundwater surveys (Adeyemo et al., 2017; Ariyo et al., 2011; Bassey et al., 2019; Fajana et al., 2019; Genedi et al., 2021; Lucy et al., 2016; Metwaly et al., 2012; Pangaribuan et al., 2017; Rizka & Satiawan, 2019).

A noteworthy aspect of the geoelectrical method in groundwater studies is the application of the one-dimensional (1D) vertical resistivity technique, commonly referred to as vertical electrical sounding (VES). The majority of these studies utilize the Schlumberger array (Adeyemo et al., 2017; Ariyo et al., 2011; Bassey et al., 2019; Fajana et al., 2019; Genedi et al., 2021; Metwaly et al., 2012; Pangaribuan et al., 2017; Rizka & Satiawan, 2019), while only a few adopt the Wenner configuration (Adeyemo et al., 2017; Lucy et al., 2016). However, as outlined by Dentith & Mudge (2014), Lowrie (2007), and Reynolds (2011), numerous other electrode configurations, including Wenner, dipole-dipole, and pole-pole arrays, can also be implemented beyond the Schlumberger arrangement.

Another important observation is that most studies focus on applying these configurations (other than Schlumberger) for subsurface profiling using two-dimensional (2D) methods, where various electrode arrays are compared. For example, Dahlin & Zhou (2004) numerically analyzed the resolution and efficiency of different electrode arrays in resistivity profiling surveys. Additionally, standard arrangements such as Wenner Alpha, Wenner-Schlumberger, and dipole-dipole arrays have been compared in various contexts, including the detection of underground cavities (Amini & Ramazi, 2017), investigation of buried concrete pipes (Abdul-Nafiu et al., 2013) or tunnels (Hassan et al., 2018), identification of bedrock over buried waste (Guedes et al., 2020), and characterization of pollutant infiltration in unconfined aquifers (Moreira et al., 2016). Among these classical electrode arrays, the dipole-dipole array is often preferred due to its sensitivity in representing subsurface targets. Also, it has a deeper depth of investigation (Szalai et al., 2009).

Conversely, limited studies were comparing vertical geoelectrical configurations. Alao et al. (2019) and Fajana et al. (2019) contrasted the Schlumberger array with its modifications in depicting subsurface information. Furthermore, Adeyemo et al. (2017) compared Wenner Alpha and Schlumberger arrays based on their output thickness measurements. Arnaut et al. (2022) simulated and conducted geoelectrical measurements using Wenner Alpha, Beta, and Gamma arrays to identify, quantify, and reduce lateral effects. Szalai et al. (2009) also studied the depth of investigation and vertical resolution from several arrays.

Given these observations, a comparative study of conventional electrode arrays for vertical geoelectrical surveys is essential to evaluate their effectiveness for shallow investigation. This study compares the Wenner Alpha, Wenner Beta, Schlumberger, and dipole-dipole configurations. Additionally, it aims to elucidate why the Schlumberger array is predominantly used in vertical geoelectrical surveys and explore the potential of other arrangements in the 1D method for describing subsurface resistivity properties.

2. Material and methods

The vertical geoelectrical method (or VES) aims to provide a vertical distribution of electrical resistivity as a function of depth below the Earth's surface (Dentith & Mudge, 2014; Lowrie, 2007; Reynolds, 2011). Typically, the electrode configurations assessed in this study include Wenner Alpha (abbreviated as WA), Wenner Beta (WB), Schlumberger (SC), and dipole-dipole (DD) arrays. Each primary array consists of four electrodes: two current electrodes (A and B) to inject electrical current into the subsurface and two potential electrodes (M and N) to measure the potential difference (ΔV) resulting from the injected current (I). The resistance (R) is calculated using the following formula:

$$R = \frac{\Delta V}{I} \tag{1}$$

To determine the observed apparent electrical resistivity (ρ_a), the measured resistance (R) is normalized by a geometrical factor (k), as described by Dentith & Mudge (2014), Lowrie (2007), and Reynolds (2011):

$$\rho_a = kR \tag{2}$$

where ρ_a is the observed resistivity (all units are in the International System).

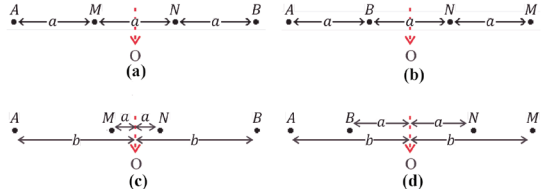

Figure 1. Electrode configuration, (a) Wenner Alpha (WA), (b) Wenner Beta (WB), (c) Schlumberger (SC), and (d) Dipole-dipole (DD) (adapted and modified from Loke, 2023).

Figure 1 illustrates the electrode positions for each array configuration. The geometrical factor (k) in Equation (2) can be derived from the electrode positions, and the general expression for it is:

$$k = 2\pi\left(\frac{1}{x_{AM}} - \frac{1}{x_{AN}} - \frac{1}{x_{BM}} + \frac{1}{x_{BN}}\right)^{-1} \tag{3}$$

with x_{AM}, x_{AN}, x_{Bm}, and x_{Bn} are the electrode spacing of AM, AN, BM, and BN, (all units are in the International System).

From Figure 1, it can be observed that the WA array has the same electrode arrangement as the SC array: *A-M-N-B*, similar to the WB array, which is equivalent to the DD array (arrangement: *A-B-N-M*). The differences lie in the electrode intervals. WA and WB arrays maintain an equal distance between their electrodes, denoted as "*a*," whereas SC and DD arrays have similar electrode spacing with specific conditions:

1. **Schlumberger (SC) Array:** In the SC array (see Figure 1(c)), the distance of *AM* must be greater than *MN*

$$x_{AM} > x_{MN} \tag{4}$$

$$\frac{1}{2}(x_{AB}) - \frac{1}{2}(x_{MN}) > x_{MN} \tag{5}$$

$$\frac{1}{2}(x_{AB}) > \frac{3}{2}(x_{MN}) \tag{6}$$

hence,

$$b > 3a \tag{7}$$

with $a > 0$ and $b > 0$.

2. **Dipole-Dipole (DD) Array:** In the DD configuration (Figure 1(d)), the *AB* interval must be smaller than *BN*

$$b < 3a \tag{8}$$

with $a > 0$, $b > 0$, and $b > a$, so Equation (8) can be rewritten as follows,

$$a < b < 3a \tag{9}$$

(all units are in the International System).

Additionally, based on Figure 1 and Equation (3), the geometrical attribute of each configuration can be expressed as follows:

$$k_{WA} = 2\pi a \tag{10}$$

$$k_{WB} = 6\pi a \tag{11}$$

$$k_{SC} = \pi\left(\frac{b^2 - a^2}{2a}\right) \tag{12}$$

$$k_{DD} = 4\pi ab\left(\frac{a+b}{(a-b)^2}\right) \tag{13}$$

where k_{WA}, k_{WB}, k_{SC}, and k_{DD} are the attributes for WA, WB, SC, and DD in sequence (all units are in the International System).

The field data acquisition process for obtaining observed resistivity in the 1D method involves measuring data from a short interval and gradually increasing the electrode spacing from the central point "O" towards both the right and left sides. This approach applies to all electrode configurations used in the vertical geoelectrical method. In this study, the maximum electrode spacing from the midpoint is 48 meters, located in the northern yard of the Engineering Laboratory Building 3 at the Sumatera Institute of Technology (Figure 2).

To analyze the subsurface resistivity variation vertically, the study utilizes Progress v3.0 software, which processes all types of electrode arrays in the vertical geoelectrical method (Antosia et al., 2022). The software's data processing follows the workflow illustrated in Figure 3. Users are only required to input the field-observed resistivity data and an initial vertical subsurface resistivity model, which is derived from analyzing the curve pattern in Figure 4. The software then automatically and iteratively performs forward and inverse modeling until the error converges, ultimately generating the final resistivity and depth models.

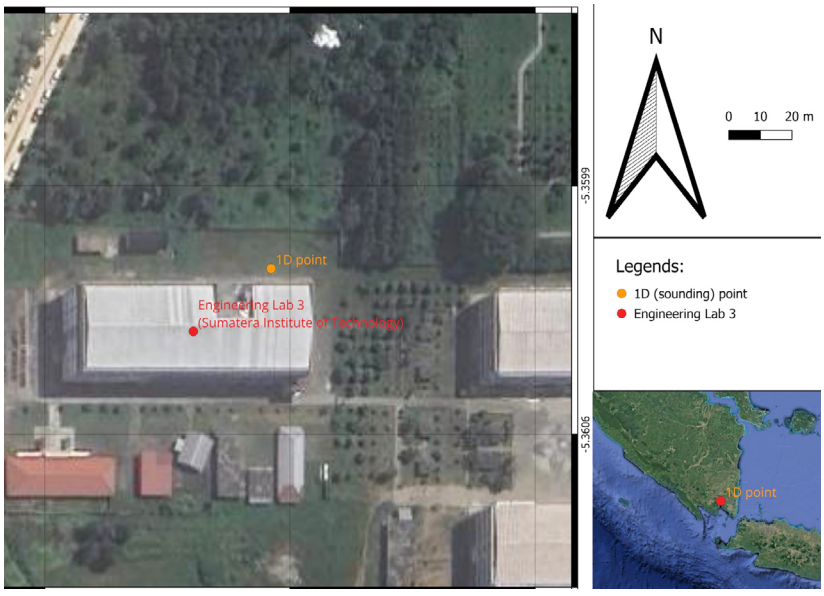

Figure 2. Measurement map of vertical electrical sounding.

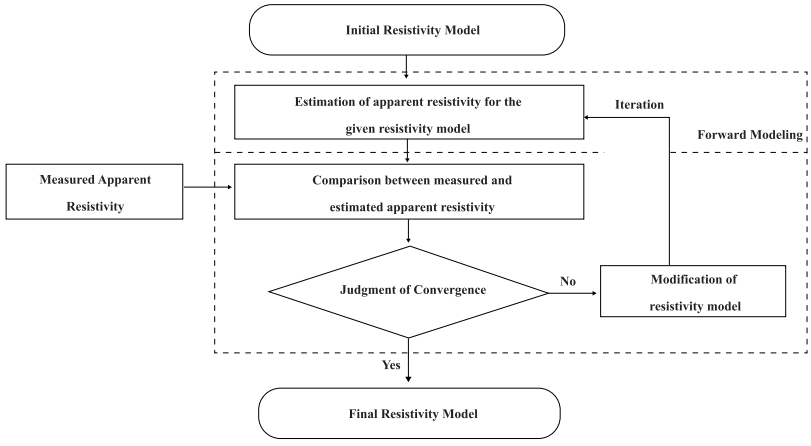

Figure 3. General flowchart of geoelectrical data processing (Aziz, 2012; Hubbard, 2009).

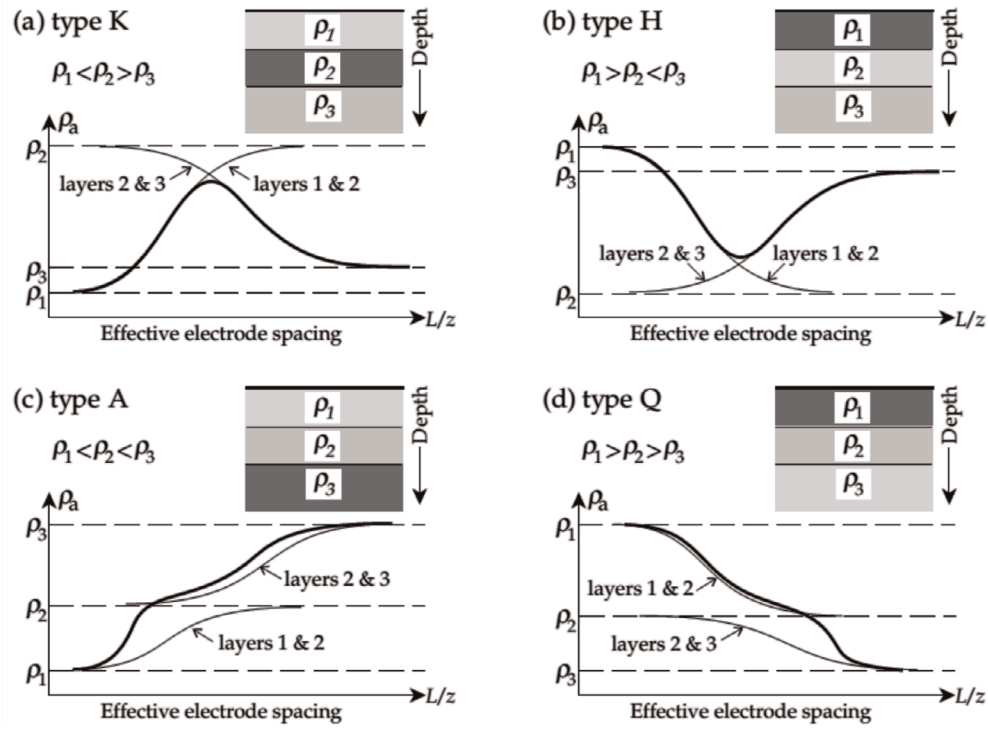

Figure 4. Theoretical three-layer sounding curves (Lowrie, 2007).

Table 1. Field vertical geoelectrical data acquisition.

L (m)	Wenner Alpha (WA)			Wenner Beta (WB)			Schlumberger (SC)			Dipole-dipole (DD)		
	a (m)	*I* (mA)	Δ*V* (mV)	*a* (m)	*I* (mA)	Δ*V* (mV)	*a* (m)	*I* (mA)	Δ*V* (mV)	*a* (m)	*I* (mA)	Δ*V* (mV)
1.5	1.0	21.14	127.20	1.0	65.16	119.89	0.5	56.67	346.45	0.5	45.10	83.25
3.0	2.0	43.47	173.56	2.0	52.32	58.04	0.5	59.42	116.42	2.0	190.17	22.53
4.5	3.0	39.04	124.40	3.0	39.24	33.22	0.5	52.59	54.93	3.5	694.35	26.90
6.0	4.0	31.51	82.94	4.0	48.59	37.17	0.5	45.87	30.17	3.0	241.15	73.10
							2.0	45.58	122.12			
7.5	5.0	33.55	76.97	5.0	43.35	31.01	2.0	51.22	91.93	4.5	242.93	35.51
9.0	6.0	45.73	91.97	6.0	47.63	31.30	2.0	48.94	62.26	6.0	262.79	20.35
12.0	8.0	50.22	79.21	8.0	35.93	20.64	2.0	51.98	38.32	9.0	994.59	25.38
15.0	10.0	45.67	57.86	10.0	43.96	21.22	2.0	46.20	21.00	9.0	1205.73	93.94
18.0	12.0	34.83	34.67	12.0	50.21	20.64	2.0	155.86	44.75	12.0	776.29	31.40
21.0	14.0	194.20	23.73	14.0	58.79	20.95	2.0	182.70	33.57	15.0	1233.09	26.41
24.0	16.0	52.02	32.33	16.0	160.38	48.03	2.0	162.02	20.66	18.0	1320.95	13.02
27.0	18.0	117.54	61.21	18.0	162.71	41.01	2.0	285.42	26.03	18.0	1356.63	23.53
30.0	20.0	231.72	30.06	20.0	159.48	33.48	2.0	511.29	33.89	21.0	1307.45	10.98
							4.0	505.20	68.34			
33.0	22.0	266.01	58.37	22.0	206.77	37.06	4.0	1013.99	97.80	21.0	1206.99	14.85
36.0	24.0	220.55	65.06	24.0	206.97	31.42	4.0	766.52	55.30	21.0	1225.72	19.01
39.0	26.0	924.89	17.14	26.0	205.71	26.28	4.0	868.45	44.94	24.0	1063.61	9.61
42.0	28.0	540.73	89.68	28.0	284.15	28.02	4.0	797.64	24.46	21.0	1227.66	12.50
45.0	30.0	542.25	92.88	30.0	302.63	27.05	4.0	751.28	22.03	24.0	1035.46	13.13
48.0	32.0	486.78	74.44	32.0	297.23	23.54	4.0	740.18	17.94	24.0	748.88	22.23

where "*a*" refers to Figure 1 for each electrode arrangement, *L* is $x_{AB}/2$ for WA and $x_{Am}/2$ for WB, $L = b$ for SC and DD.

3. Results and discussion

A. Field Measurement and Data Acquisition

Field measurements were conducted using the ARES instrument from GF Instruments to compare each electrode configuration. The data acquisition parameters were standardized across all arrays, including a maximum power of 600 W, four data stackings, and a minimum measured potential of 20 mV. The electrode distance (*L*) from the midpoint to the outer electrode was consistent for all arrays. Table 1 summarizes the field data acquisition for the vertical geoelectrical technique.

Observations:

1. Current (I): the injected current increases with electrode distance across all arrays to maintain the minimum voltage reading of 20 mV (Figure 5(a)).
2. Voltage difference (ΔV): the potential response decreases as the distance between the current and potential electrodes increases (Figure 5(b)).
3. Dipole-dipole (DD) array: several voltage values did not achieve the minimum setting for $L > 27$ m despite a higher injected current than other configurations. This indicates challenges in maintaining voltage readings over larger distances with the DD array (see Figure 5(a)).
4. Schlumberger (SC) array: maintains better potential readings as the electrodes remain within AB the perimeter, reducing voltage attenuation (Figure 5(b)).
5. Wenner Alpha (WA) array: demonstrates more stable voltage readings due to consistent electrode spacing (Figure 5(b)).

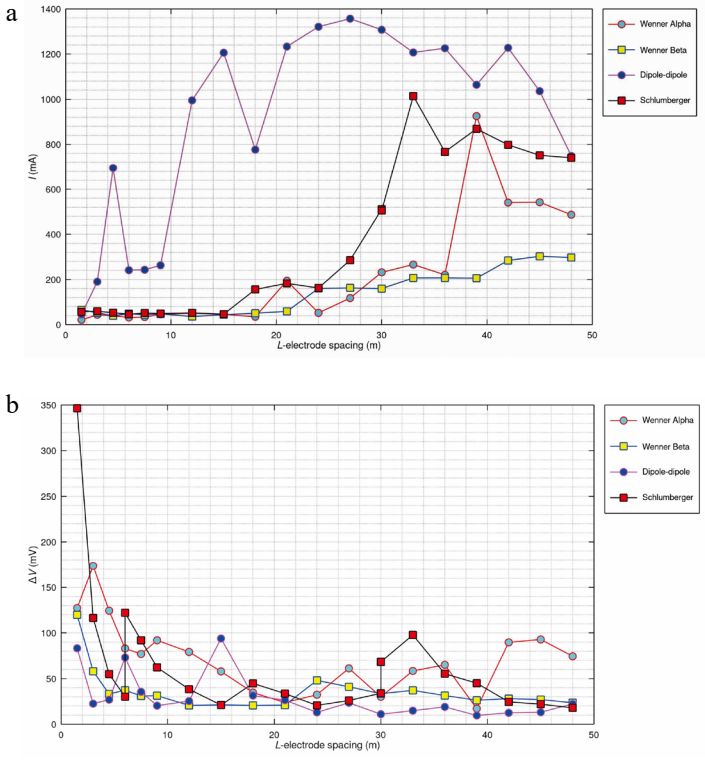

Figure 5. Measured electrical parameters over the electrode distance "L," (a) current, and (b) voltage difference.

B. Quantitative Analysis of Electrode Configurations

To substantiate the claims regarding the arrays' performance, specific quantitative metrics were analyzed:

1. Average electrical current and voltage

The initial analysis involves computing the average value of the raw data from Table 1, and the results are shown in the following table.

Table 2. The average value of electrical current and voltage for all arrays.

Parameter	WA	WB	SC	DD
I (mA)	206.41	130.06	342.81	862.08
ΔV (mV)	73.35	36.31	65.39	30.40
The ratio I of and ΔV	2.81	3.58	5.24	28.36

a. Current ratio: the WA requires approximately 2.81 mA to achieve the same voltage reading as DD, indicating higher efficiency in current usage.

b. Voltage response: the WA exhibits a more stable and higher voltage response than DD, which shows the lowest voltage readings.

These observations reinforce the earlier explanation that WA demonstrates greater stability and consistency in measuring voltage response, indicating superior signal strength. For clarity, the signal strength is categorized into three levels: high, moderate, and low. Consequently, WA falls into the high category, followed by WB and SC with moderate strength, while DD has the lowest.

2. Apparent resistivity calculations

Using Equations (1), (2), and (10)-(13), the resistivities for each electrode configuration were calculated and plotted, presented in Figure 6.

a. Apparent resistivity trends: all configurations show similar trends, fluctuating resistivity values as electrode spacing increases. However, the DD array exhibits more variability, suggesting lower reliability in resistivity measurements (Figure 6(a)).

b. Cumulative apparent resistivity: the cumulative resistivity plot clearly highlights deviations. The WB, SC, and DD arrays show more consistency compared to WA and follow a similar increasing pattern (Figure 6(b)).

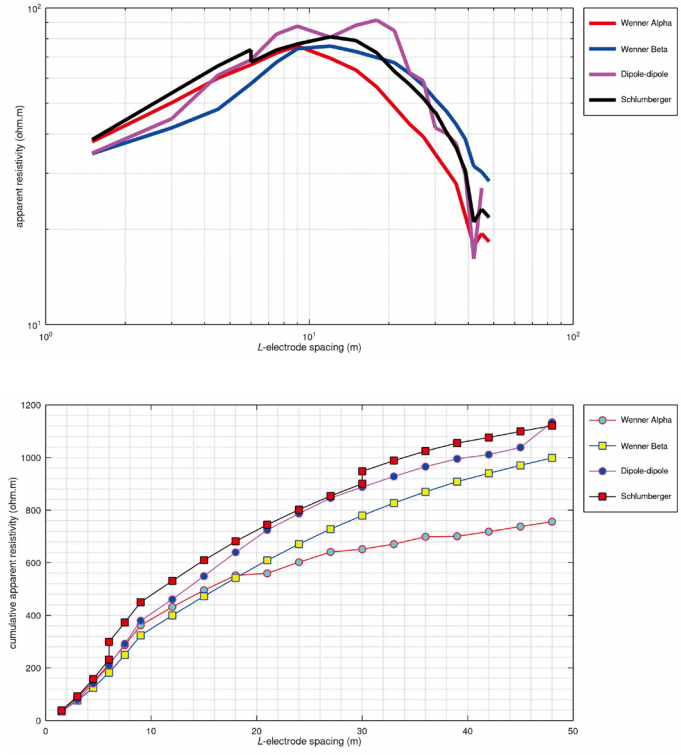

Figure 6. Observed data over electrode spacing "L," (a) apparent resistivity, and (b) cumulative apparent resistivity.

3. Modeling and inversion

Next, the output comparison was performed by processing data through the Progress v3.0 software. Erenow, the initial model must be inserted into the software. It was determined by curve pattern analysis in Figure 4. Based on the observed curve in Figure 6(a), the resistivity model may composite two curve shapes, "K" and "Q" types. It contains four resistivity layers with the following conditions, $\rho_1 < \rho_2 > \rho_3 > \rho_4$, where ρ_1, ρ_2, ρ_3, and ρ_4 are resistivity estimations at the first, second, third, and fourth layers in sequence. Its initial model is shown in the following table.

Table 3. Initial resistivity and depth models.

Layer	Depth (m)	Resistivity (ohm.m)
1	0	30
2	1.5	100
3	10	50
4	30	20

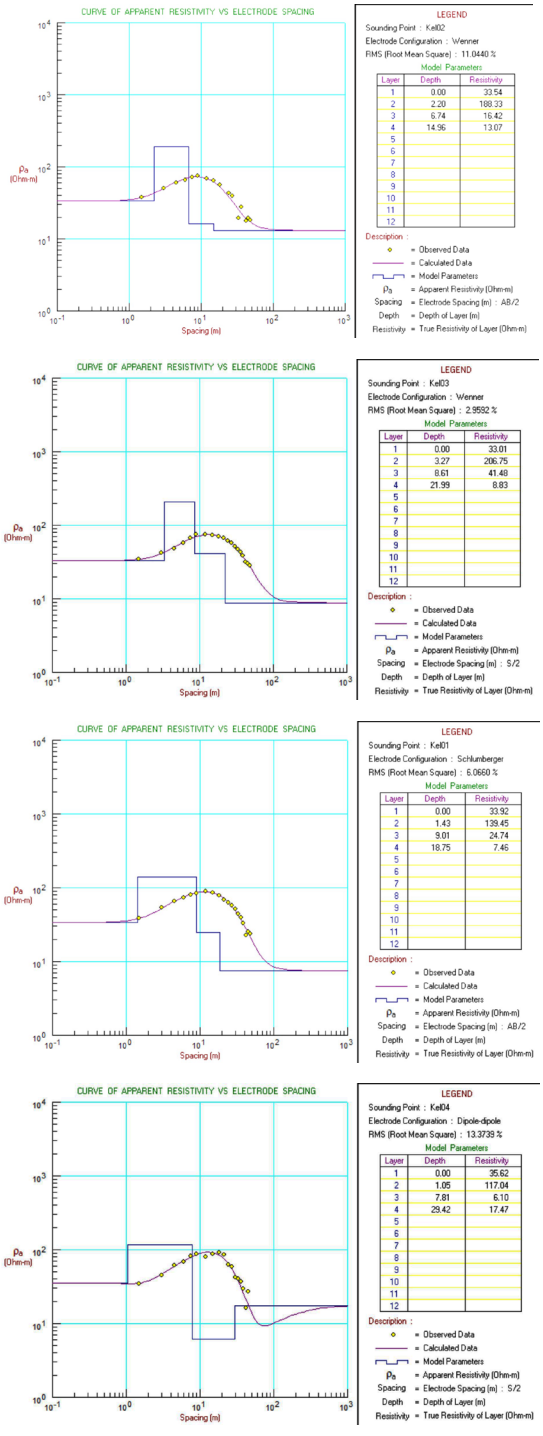

Figure 7. Data processing result: (a) WA, (b) WB, (c) SC, and (d) DD.

The generated outputs of each array from the software are displayed in Figure 7. Their results are generally identical, except in the DD, the resistivity value in the fourth layer becomes higher than in the third layer; its curve pattern is changed to the "KH" type.

a. **WA and WB arrays:** display more stable and consistent resistivity profiles that align with geological expectations.
b. **SC array:** shows slight variations but maintains consistency in resistivity measurements.
c. **DD array:** exhibits fluctuating resistivity values, particularly in deeper layers, indicating potential inaccuracies.

The results in Table 4 represent the final models of the vertical resistivity properties beneath the earth's surface in the study area, accompanied by the following explanation:

a. **Layer 1:** consistent resistivity across all arrays, indicating reliable detection of the near-surface layer.
b. **Layer 2:** all arrays show high resistivity values with lower standard deviations, indicating more reliable measurement. However, the deviation for depth value is the highest.
c. **Layer 3:** the WA and DD arrays exhibit lower resistivity values, suggesting less consistency, possibly leading to geological misinterpretations. The depth of this layer tends not to vary across configurations.
d. **Layer 4:** the WA and DD arrays have similar resistivity values, as do WB and SC. This similarity may lead to the same geological interpretation. Besides, DD exhibits greater depth penetration, aligning with the findings of Szalai et al. (2009). Therefore, it can be concluded that DD has the highest depth of investigation, WA has the lowest, and the remaining two arrays fall within a moderate depth range.

Table 4. Subsurface resistivity and depth estimation for all electrode arrangements.

WA		WB		SC		DD		Mean			
Depth h (m)	ρ (ohm.m)	Depth h (m)	ρ (ohm.m)	Depth h (m)	ρ (ohm.m)	Depth h (m)	ρ (ohm.m)	Depth h (m)	ρ (ohm.m)	Depth h (m)	ρ (ohm.m)
0.00	33.54	0.00	33.01	0.00	33.92	0.00	35.62	0.00	0	34.02	2.87
2.20	188.33	3.27	206.75	1.43	139.45	1.05	117.04	1.99	42.69	162.89	22.18
6.74	16.42	8.61	41.48	9.01	24.74	7.81	6.10	8.04	10.78	22.19	58.37
14.96	13.07	21.99	8.83	18.75	7.46	29.42	17.47	21.28	24.99	11.71	33.46

4. Convergence analysis

The convergence of the inversion process was evaluated using the RMS misfit values. It is shown in Figure 8.

a. **WB array:** lowest RMS misfit, indicating the best fit between observed and modeled data.
b. **SC array:** moderate RMS misfit, still within acceptable ranges.
c. **WA array:** higher RMS misfit than WB and SC but within acceptable limits.
d. **DD array:** highest RMS misfit, suggesting less accurate modeling.

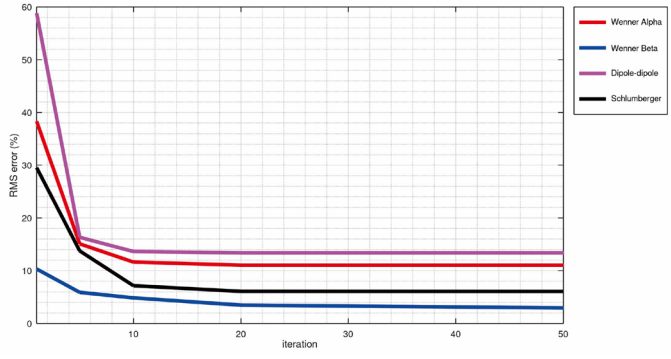

Figure 8. Convergence RMS error for all configurations.

5. Subsurface geological interpretation

The subsurface rock features are obtained and referred to in the study of Rizka & Satiawan (2019) because of the same geological formation. As a result, the particular configuration has a different delineation (Table 5).

a. **Near-surface layers (layers 1-2):** consistent interpretation across all arrays.
b. **Intermediate layers (layer 3):** the WA and DD arrays interpret the third layer as tuffaceous clay, whereas WB and SC arrays interpret it as tuffaceous sand.

c. Deep layers (layer 4): all arrays consistently interpret the fourth layer as tuffaceous clay, although there is a discrepancy in resistivity values.

These disparities, particularly in layer 3, may be attributed to the DD array's lower signal strength and higher variability, as well as potential horizontal property influences in the WA array. The WB and SC arrays provide more reliable interpretations due to their consistent resistivity measurements and lower variability.

Table 5. Estimating subsurface geological properties refers to Rizka & Satiawan (2019).

WA		WB		SC		DD	
ρ (ohm.m)	Rock type	ρ (ohm.m)	Rock type	ρ (ohm.m)	Rock type	ρ (ohm.m)	Rock type
33.54	Tuffaceous sand	33.01	Tuffaceous sand	33.92	Tuffaceous sand	35.62	Tuffaceous sand
188.33	Tuff	206.75	Tuff	139.45	Tuff	117.04	Tuff
16.42	Tuffaceous clay	41.48	Tuffaceous sand	24.74	Tuffaceous sand	6.10	Tuffaceous clay
13.07	Tuffaceous clay	8.83	Tuffaceous clay	7.46	Tuffaceous clay	17.47	Tuffaceous clay

6. Sensitivity and resolution analysis

Szalai et al. (2009) stated that high resolution generally means sensitivity is concentrated in a smaller depth, while high sensitivity often extends deeper but with lower resolution. A previous study by Abbas (2017) reported that WA has the highest resolution while DD has the lowest (Figure 9). Therefore, based on this study, it can be concluded that::

a. Resolution capacity: the WA array offers the highest vertical resolution, followed by SC and WB arrays. The DD array has the lowest resolution, limiting its effectiveness in accurately delineating subsurface layers.

b. Sensitivity patterns: this parameter contrasts with the previous one, meaning the DD array demonstrates the highest vertical sensitivity, allowing for improved detection of deeper subsurface features. The SC follows it, while the WB array exhibits moderate sensitivity, and the WA array has the lowest sensitivity.

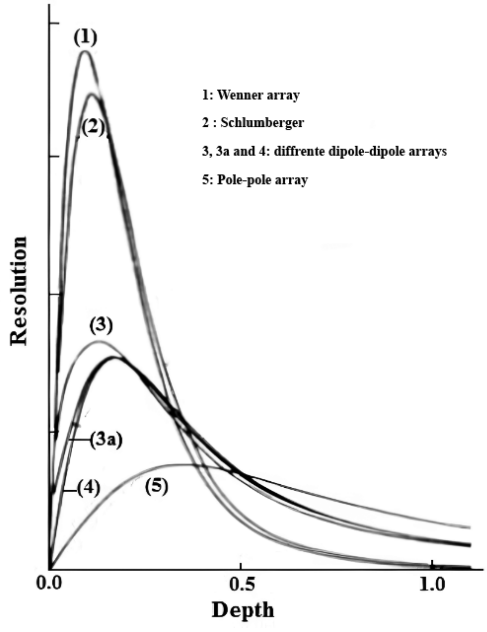

Figure 9. Sensitivity pattern diagram (Abbas, 2017).

Based on this study's analysis, four key parameters are considered when selecting an electrode arrangement for vertical geoelectrical surveys: signal strength, vertical sensitivity, resolution, and the representative depth of investigation. Overall, as shown in Table 6, WB and SC perform better in delineating the subsurface properties than the other two. This study testifies that the Schlumberger (SC) array is the most widely used in the 1D method. Moreover, a viable alternative electrode mode can be considered a vertical geoelectrical array, Wenner Beta (WB).

Table 6. Vertical geoelectrical parameters of each electrode configuration.

Parameter	WA	WB	SC	DD
Signal strength	high	moderate	moderate	low
Vertical sensitivity	low	moderate	moderate	high
Vertical resolution	high	moderate	moderate	low
Depth of investigation	low	moderate	moderate	high

Conclusion

This study analyzed the performance of different electrode configurations in the vertical resistivity method to assess their effectiveness in delineating subsurface features. Four configurations were evaluated: Wenner Alpha (WA), Wenner Beta (WB), Schlumberger (SC), and dipole-dipole (DD).

1. **Wenner Beta (WB) and Schlumberger (SC) arrays:** demonstrated better performance in all parameters. Additionally, these arrays exhibited lower standard deviations in resistivity measurements, indicating higher reliability and consistency.
2. **Wenner Alpha (WA) array:** showed above-average performance in signal strength and vertical resolution but had lower vertical sensitivity compared to other arrays. Despite some variability in resistivity measurements, the WA array maintained stable voltage readings.
3. **Dipole-Dipole (DD) array:** while sensitive vertically and effectively representing subsurface resistivity, it required more power and exhibited significant discrepancies in resistivity patterns, particularly in deeper layers. This led to potential geological misinterpretations, making it less reliable for accurate subsurface delineation.

Overall, the WB and SC arrays proved more effective for 1D resistivity surveys due to their enhanced performance metrics. However, the study's limitation to a 100-meter measurement length necessitates further research with extended ranges to confirm the scalability and generalizability of these findings.

Acknowledgments

The author expresses gratitude to the Geophysical Engineering students and laboratory technicians for assisting in data acquisition for this study. Appreciation is also extended to the reviewers for their valuable and constructive feedback on this article.

References

Abbas, M. (2017). *Development of a geophysical and geochemical methodology for the characterization of hydrocarbon contamination of soil and groundwater*. https://tel.archives-ouvertes.fr/tel-01820616

Abdul-Nafiu, A. K., Nordin, M. N. Mohd., Abdullah, K., Saheed, I. K., & Abdulrahman, A. (2013). Effects of Electrode Spacing and Inversion Techniques on the Efficacy of 2D Resistivity Imaging to Delineate Subsurface Features. *American Journal of Applied Sciences*, *10*(1), 64–72. https://doi.org/10.3844/ajassp.2013.64.72

Adeyemo, I. A., Ojo, B. T., & Raheem, W. O. (2017). Comparison of Thickness and Depth Resolution Power of Wenner and Schlumberger Arrays: A Case Study of Temidire Quarters, Akure, Nigeria. *Journal of Geoscience and Environment Protection*, *05*(03), 233–239. https://doi.org/10.4236/gep.2017.53016

Alao, J. O., Dogara, M. D., Danlami, A., & Samson, E. E. (2019). Comparative Assessment of half Schlumberger Configuration as an Alternative

Method to the Conventional Schlumberger Configuration at Trade Centre, Mani-Nissi Village, Kaduna, Nigeria. *International Journal of Applied Physics*, *6*(3), 51–56. https://doi.org/10.14445/23500301/ijap-v6i3p109

Al-Saady, H. A., Karim, H. H., & AL-Menshed, F. H. (2022). Comparison of Three Electrical Resistivity Arrays to Investigate Weak Zones in Soil, along a Profile Southeast Baghdad City, Iraq. *Iraqi Journal of Science*, *63*(11), 4793–4798. https://doi.org/10.24996/ijs.2022.63.11.18

Amini, A., & Ramazi, H. (2017). CRSP, numerical results for an electrical resistivity array to detect underground cavities. *Open Geosciences*, *9*(1), 13–23. https://doi.org/10.1515/geo-2017-0002

Antosia, R. M., Mustika, Putri, I. A., Rasimeng, S., & Dinata, O. (2021). Andesite prospect at West Sungkai of North Lampung: Its distribution based on electrical resistivity tomography. *IOP Conference Series: Earth and Environmental Science*, *882*(1), 012086. https://doi.org/10.1088/1755-1315/882/1/012086

Antosia, R. M., Putri, I. A., Farduwin, A., Irawati, S. M., & Santoso, N. A. (2022). Peninjauan Ulang Kedalaman Akuifer Menggunakan Metode Resistivitas 1D di Desa Gayau, Kabupaten Pesawaran. *Jurnal Abdi Masyarakat Indonesia*, *2*(2), 651–660. https://doi.org/10.54082/jamsi.309

Arifin, M. H., Kayode, J. S., Izwan, M. K., Zaid, H. A. H., & Hussin, H. (2019). Data for the potential gold mineralization mapping with the applications of Electrical Resistivity Imaging and Induced Polarization geophysical surveys. *Data in Brief*, *22*, 830–835. https://doi.org/10.1016/j.dib.2018.12.086

Ariyo, S. O., Folorunso, A. F., & Ajibade, O. M. (2011). Geological and geophysical evaluation of the Ajana area's groundwater potential, southwestern Nigeria. *Earth Sciences Research Journal*, *15*(1), 35–40.

Arnaut, F., Sretenović, B., & Cvetkov, V. (2022). Improvement of 1D geoelectric sounding by narrowing the equivalence range and identification, quantification and reduction of lateral effects using the tri-potential technique. *Geofizika*, *39*(2), 297–320. https://doi.org/10.15233/gfz.2022.39.15

Aziz, N. A. (2012). *Three Dimension Electrical Resistivity and IP Imaging for Soil Layers Investigation at UoT-Baghdad* [University of Technology]. https://www.researchgate.net/publication/311805163

Bassey, P., Lawrence, O. O., & Ailego, J. (2019). Geo-electrical Resistivity Evaluation of Groundwater Potential at University Of Benin Ugbowo Campus, Benin-City, Edo State of Nigeria, Using the Schlumberger Array. *Journal of Applied Sciences and Environmental Management*, *23*(9), 1761–1770. https://doi.org/10.4314/jasem.v23i9.23

Dahlin, T., & Zhou, B. (2004). A numerical comparison of 2D resistivity imaging with 10 electrode arrays. *Geophysical Prospecting*, *52*(5), 379–398. https://doi.org/10.1111/j.1365-2478.2004.00423.x

Dentith, M., & Mudge, S. (2014). *Geophysics for the Mineral Exploration Geoscientist*. Cambridge University Press .

Fajana, A. O., Sanuade, O. A., Olawunmi, O. T., & Oyebamiji, A. R. (2019). Comparison of Conventional Schlumberger and Modified Schlumberger Arrays in Estimating Aquifer Parameters in A Typical Basement Complex, Southwestern Nigeria. *FUOYE Journal of Engineering and Technology*, *4*(1), 92–96. https://doi.org/10.46792/fuoyejet.v4i1.306

Farduwin, A., Lumbatoruan, P. G., Karyanto, & Triyanto, D. (2021). Identification of zeolite using electrical resistivity tomography in Campang Tiga, South Lampung Regency. *IOP Conference Series: Earth and Environmental Science*, *882*(1), 012046. https://doi.org/10.1088/1755-1315/882/1/012046

Farooq, M., Park, S., Song, Y. S., Kim, J. H., Tariq, M., & Abraham, A. A. (2012). Subsurface cavity detection in a karst environment using electrical resistivity (er): A case study from Yongweol-ri, South Korea. *Earth Sciences Research Journal*, *16*(1), 75–82.

Fernandes, S., Santos, D., Moreira, C. A., Gomes Rosa, F. T., Borssatto, K., & Aparecida Da Silva, M. (2018). Geoelectric Prospection of Copper Occurrence in Folded Structures in the Sul-Riograndense Shield (Brazil). *Revista Brasileira de Geofísica*, *36*(3), 245–254. www.scielo.br/rbg

Genedi, M., Ghazala, H., Mohamed, A., Massoud, U., & Tezkan, B. (2021). Lateral Constrained Inversion of DC-Resistivity Data Observed at the Area North of Tenth of Ramadan City, Egypt for Groundwater Exploration. *Geosciences (Switzerland)*, *11*(6), 248. https://doi.org/10.3390/geosciences11060248

Guedes, V. J. C. B., Lima, V. B. de O., Borges, W. R., & da Cunha, L. S. (2020). Comparison of the Geoelectric Signature with Different Electrode Arrays at the Jockey Club Landfill of Brasília. *Revista Brasileira de Geofisica*, *38*(1), 41–51. https://doi.org/10.22564/rbgf.v38i1.2034

Hassan, A. A., Kadhim, E. H., & Ahmed, M. T. (2018). Performance of Various Electrical Resistivity Configurations for Detecting Buried Tunnels Using 2D Electrical Resistivity Tomography Modelling. *DJES*, *11*(3), 14–21. https://doi.org/10.24237/djes.2018.11303

Hubbard, J. L. (2009). *Use of Electrical Resistivity and Multichannel Analysis of Surface Wave Geophysical Tomography in Geotechnical Site Characterization of Dam*. The University of Texas at Arlington.

Loke, M. H. (2023). *Tutorial : 2-D and 3-D electrical imaging surveys*. https://www.geotomosoft.com/coursenotes.zip

Lowrie, W. (2007). Fundamentals of Geophysics. In *Cambridge University Press* (Second Edition). Cambridge University Press.

Lucy, M., Willis, A., John, G., & Hezekiah, C. (2016). Geophysical Investigation and Characterization Of Groundwater Aquifers In Kangonde Area, Machakos County In Kenya Using Electrical Resistivity Method. *IOSR Journal of Applied Geology and Geophysics*, *4*(2), 23–35.

Metwaly, M., Al-Awadi, E., Shaaban, S., Al-Fouzan, F., Al-Mogren, S., & Al-Arifi, N. (2012). Groundwater exploration using geoelectrical resistivity technique at Al-Quwy'yia area central Saudi Arabia. *International Journal of Physical Sciences*, *7*(2), 317–326. https://doi.org/10.5897/IJPS11.1659

Moreira, C. A., Lapola, M. M., & Carrara, A. (2016). Comparative analyzes among electrical resistivity tomography arrays in the characterization of flow structure in free aquifer. *Geofisica Internacional*, *55*(2), 119–129. https://doi.org/10.22201/igeof.00167169p.2016.55.2.1716

Ojo, J. S., Olorunfemi, M. O., & Falebita, D. E. (2011). An appraisal of the geologic structure beneath the Ikogosi warm spring in South-Western Nigeria using integrated surface geophysical methods. *Earth Sciences Research Journal*, *15*(1), 27–34.

Pangaribuan, A. F., Mohammad, F., Fadly, M., & Muttaqin, D. Z. (2017). Aquifer Distribution Based on 1D Resistivity Method at Jatinangor Educational Area, Sumedang Regency, West Java Province. *IOP Conference Series: Earth and Environmental Science*, *62*(1), 012041. https://doi.org/10.1088/1755-1315/62/1/012041

Reynolds, J. M. (2011). *An Introduction to Applied and Environmental Geophysics* (2nd Edition). John Wiley & Sons, Ltd. www.wiley.com/go/reynolds/introduction2e

Rezaei, S., Shooshpasha, I., & Rezaei, H. (2018). Empirical correlation between geotechnical and geophysical parameters in a landslide zone (Case study: Nargeschal landslide). *Earth Sciences Research Journal*, *22*(3), 195–204. https://doi.org/10.15446/esrj.v22n3.69491

Rizka, & Satiawan, S. (2019). Investigasi Lapisan Akuifer Berdasarkan Data Vertical Electrical Sounding (VES) dan Data Electrical Logging; Studi Kasus Kampus Itera. *Bulletin of Scientific Contribution: GEOLOGY*, *17*(2), 91–100. http://jurnal.unpad.ac.id/bsc

Szalai, S., Novák, A., & Szarka, L. (2009). Depth of investigation and vertical resolution of surface geoelectric arrays. *Journal of Environmental and Engineering Geophysics*, *14*(1), 15. https://doi.org/10.2113/JEEG14.1.15